ACS APPLIED MATERIALS & INTERFACES

Article

Polydopamine Thin Films as Protein Linker Layer for Sensitive Detection of Interleukin-6 by Surface Plasmon Enhanced Fluorescence Spectroscopy

Mana Toma, and Keiko Tawa

ACS Appl. Mater. Interfaces, **Just Accepted Manuscript** • DOI: 10.1021/acsami.6b06917 • Publication Date (Web): 02 Aug 2016

ACS Publications

ACS Applied Materials & Interfaces is published by the American Chemical Society.
1155 Sixteenth Street N.W., Washington, DC 20036

Polydopamine Thin Films as Protein Linker Layer for Sensitive Detection of Interleukin-6 by Surface Plasmon Enhanced Fluorescence Spectroscopy

*Mana Toma, Keiko Tawa**

Department of Applied Chemistry for Environment, School of Science and Technology, Kwansei Gakuin University, Sanda, Japan 669-1337.

KEYWORDS: Polydopamine, biosensor, surface plasmon enhanced fluorescence, surface chemistry, Interleukin-6.

ABSTRACT

Polydopamine (PDA) thin films are introduced to the surface modification of biosensor surfaces utilizing surface plasmon enhanced fluorescence spectroscopy (SPFS), as the linker layer of capture antibody on to the sensor surfaces. The capture antibody can be directly attached to the sensor surface without using any coupling agent by functionalizing the gold sensor surface with PDA thin films. The PDA coating is performed by a single step preparation process by applying the dopamine solution on the sensor surface, which requires extremely short incubation time (10 min). The real time, in-situ measurement of the adsorption kinetics of the capture antibody onto

the PDA coated sensor surface is studied by surface plasmon resonance (SPR) spectroscopy. It reveals that the immobilization of capture antibody immediately occurs after introduction of a solution containing capture antibody, and the sensor surface is fully covered with the capture antibody. The sensitive detection of the cytokine marker Interleukin-6 (IL-6) is performed by SPFS using a sandwich assay format with fluorescently labeled detection antibody. The sensor chips functionalized by PDA chemistry exhibited sensitive sensor responses with low non-specific adsorption of the detection antibody onto the sensor surface. The detection limit of the IL-6 with the developed SPFS biosensor is determined to be 2 pg/mL (100 fM), which is within the range of the diagnostic criteria. Our observation elucidates the remarkable utility of PDA coatings for the chemical modifications of the metallic sensor surfaces by a simple, brief and inexpensive manner.

INTRODUCTION

Over the last years, the biosensors have emerged as important analytical tools of the biomolecules in the various fields, such as clinical diagnostic, food safety and environmental monitoring.[1] Among others, the fluorescence biosensors employing signal amplification strategies based on surface plasmon enhanced fluorescence (SPF) and surface plasmon coupled emission (SPCE) have attracted great attentions due to their excellent ability for the rapid and sensitive detection of the target analyte.[2, 3] For SPF biosensors utilizing propagating surface plasmons, a glass or plastic substrate coated with a thin metal film is used for the excitation of surface plasmon resonance (SPR). The enhanced electromagnetic field induced by the resonantly excitation of the surface plasmons in the vicinity of the metal surface is utilized for the amplified

excitation of the fluorophores by using e.g. sandwich assay format with fluorescently labeled detection antibodies. Up to now, the sensitive detection of various biomolecules including biomarkers,[4-9] pathogens,[10, 11] food toxins[12] and nucleotides[13] have been demonstrated by using SPFS biosensors. Although the sensing performance of the SPF biosensors highly depends on the surface plasmon modes and the surface architectures, many of them have achieved femto molar (fM) level detections of the target molecules.[2] In the plasmonic biosensors including SPFS biosensors, the sensor surfaces consisting of metal or metal coated with oxide need to be modified with the bio-recognition elements (BREs), such as antibodies,[4-8, 10, 12] nucleotides,[13] aptamers,[14] and molecular imprinted polymers,[15, 16] for the affinity binding of the target analyte. The linker layers are typically used for the stable attachment of the BREs on to the sensor surfaces. A variety of surface chemistries has been proposed to maintain the density and the direction of BREs, and the anti-fouling properties of the sensor surface. Alkanethiols and silane coupling agents with functional tailor groups are widely used for the immobilization of BREs on the sensor surfaces, as these molecules formed nicely controlled self-assembled monolayers (SAMs). Dextran matrix and hydrogel binding matrix have been used in order to increase the amount of the immobilized BREs and improve the anti-fouling properties of the sensor surfaces.[4, 12, 17] Protein linker layers, such as streptavidin, protein A and s-layer are also used to control the density and the direction of attached BREs.[18-21] In the commonly used surface modification processes, the sensor surfaces are firstly functionalized with thiol SAMs, then additional polymer layers or protein layers are anchored. In general, the BREs such as capture antibody are covalently bound to the carboxylated sensor surfaces by amine coupling through 1-Ethyl-3-(3-dimethylaminopropyl)carbodiimide (EDC) and N-hydroxysuccinimide (NHS) chemistry. The functionalization of the surface with thiol molecules is typically performed overnight process,

and requires multistep pretreatment for the binding of BREs, which makes the sample preparation process time consuming. In addition, the used chemicals for these surface chemistries are generally expensive or synthesized in special laboratories. The effort for the rapid surface modifications was reported by utilizing the bispecific antibodies that specifically bind to the substrate and the target molecules,[6] nevertheless, the application of such bispecific antibodies is still limited.

Here, we propose a simple, rapid and cost effective modification method of the SPFS biosensor surfaces by employing the mussel inspired polydopamine (PDA) thin films as the linker layer of the antibodies. PDA is known as the biomimetic adhesive materials which can be coated on any kind of materials by simply applying the dopamine solutions onto the surfaces.[22] In addition to its notable chemical properties, the simplicity of the surface modification process and the easy availability of the chemicals make PDA coating techniques attractive. Up to now, various applications of PDA coated surfaces have been proposed, which are including cell adhesion,[23] control wettability of surfaces,[24] anti-biofouling surfaces,[25] and biosensors.[26, 27] One of the remarkable advantages of the PDA coated surfaces is their availability for the binding of biomolecules through amino groups and thiol groups without using any coupling agent.[28] Recently, DNA microarrays were fabricated on the gold surfaces by using PDA thin films as the linker layer of the amine terminated DNA onto the sensor surface, and the sensitive detection of DNA hybridization was reported with the surface plasmon resonance imager.[26, 29] Shi *et al.* reported improved sensor responses of optical fiber SPR biosensor with model immunoassay by functionalizing the sensor surface with PDA thin films.[27] In this study, we fabricated PDA coated SPFS biosensor chips, and characterized the surface by means of adsorption kinetics of the capture antibody, amount of the immobilized capture antibody and the sensing performance. The

SPFS sensor surfaces were functionalized with PDA thin films by simply applying dopamine solution for a short incubation time. Further, direct attachment of the capture antibody on the sensor surface was demonstrated. As the target analyte, interleukin-6 (IL-6) was detected by using sandwich immunoassay. IL-6 is known as one of cytokines relating inflammatory and autoimmune activities, and has been used as a biomarker for clinical diagnostics of inflammatory and infection diseases such as sepsis,[30] Castleman's disease,[31] and Rheumatoid Arthritis.[32] It has been reported that the plasma level of IL-6 of healthy persons are 1-5 pg/mL.[32, 33] The risks of these diseases increased when the plasma concentration of IL-6 is elevated. In our laboratory, the sensitive detection of Il-6 with the limit of detection (LOD) of 2 pg/mL (100 fM) was performed by using plasmonic chip, which is a metal coated diffraction grating supporting grating coupled surface plasmon resonance, and SPF imaging with sandwich immunoassay.[8] By using the PDA coated sensor chips, the limit of detection of IL-6 was determined to be 100 fM, which is comparable to that obtained by using conventional surface chemistry and SPF imaging technique, and within the range of the clinically relevant value. PDA chemistry enables us to functionalize the SPFS biosensor surface with biomolecules by extremely short and simple process without sacrificing the detection sensitivity.

EXPERIMENTAL SECTION

Materials

All the chemicals were used as received. Recombinant human IL-6 (570806), two kinds of purified anti-human IL-6 antibody (clone MQ2-13A5 and MQ2-39C3 for capture and detection antibodies, respectively) and the blocking agent composed of phosphate buffered saline (PBS) solution and bovine serum (ELISA assay diluent, 421203) were purchased from Biolegend. The

blocking buffer was prepared from five times dilution of the purchased blocking agent with PBS. The detection antibody was labeled with Alexa fluor 647 by using the labelling kit from Thermo Fisher scientific. The labeling ratio was determined to be 2.6 by UV-Vis absorption spectroscopy.10 mM Tris buffer (pH=8.5) was prepared by mixing 10 mM tris(hydroxymethyl)aminomethane solution and 10 mM Tris(hydroxymethyl)aminomethane solution. The buffer salts of Tris buffer were purchased from Nacalai tesque. Phosphate buffered saline (PBS) was prepared with a PBS tablet and MilliQ water. PBS-tween (PBST) was prepared by adding 0.05 v% of Tween 20 into PBS buffer. All other chemicals were obtained from Sigma Aldrich.

Sensor Chip Fabrication

The fabrication process of the sensor chip is schematically described in Figure 1. The high refractive index LaSFN9 glass (SCHOTT) was used as the substrate. A thin gold film was deposited on the LaSFN9 glass by RF sputtering. The thickness of metal layer was about 47 nm measured by SPR spectroscopy. PDA coating was performed by following the procedure reported previously.[26] 2 mg/mL dopamine solution in Tris buffer (10 mM, pH8.5) was applied to the sensor surface for 10 min, followed by rinsing with MilliQ water and drying with N_2 stream. In this condition, the thickness of PDA layer in dry state is about 1.3 nm.[26] Let us note that the thickness of PDA layer can be controlled by the deposition time.[22, 26, 34] The PDA coated sensor chips were kept in the vacuum desiccator until the immobilization process of the capture antibody was performed.

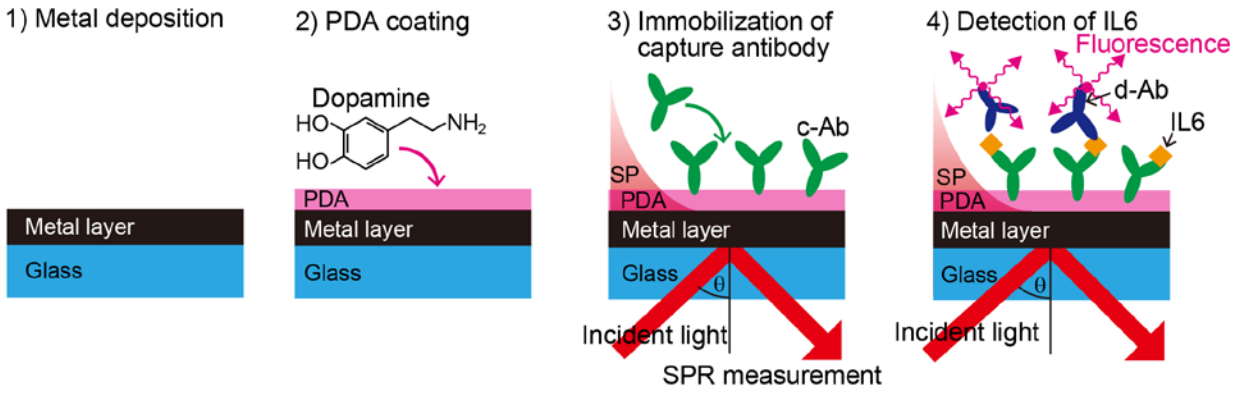

Figure 1. Schematic drawings of the sample preparation process and the detection assay. 1) Deposition of a gold thin film. 2) PDA coating. 3) Immobilization of capture antibody. 4) Detection of IL-6 by sandwich immunoassay with fluorescently labeled detection antibody.

Optical Setup

A home-build optical setup based on the attenuated total reflection (ATR) method with Krestchmann configuration was used for the angular reflectivity measurement and fluorescence intensity measurement, as shown in Figure S1 in the supporting information. The laser beam from He-Ne laser (λ=632.8 nm, 05-LHP-151, Melles Griot) passed the chopper and polarizers before made an incident to the sensor chip. A set of polarizers were used to adjust the laser beam intensity and to make the incident light p-polarized. The sensor chip was attached to the 90º LaSFN9 prism with refractive index matching oil. The prism head was mounted on the two axes motorized rotation stage (SGSP-120YAW-W, Sigma Koki) which was used to control the angle of incident θ and the detection angle for the reflectivity measurement at 2θ. The intensity of the reflected laser beam was detected by using the chopper and the photodiode with the lock-in amplifier (7265, PerkinElmer). The fluorescence light emitting into the direction of the aqueous solution were collected by using a set of lenses (AC254-040-A-ML and AC245-06-A, Thorlabs)

and filters (FL670-10, Tholabs, and BLP01-635R-25, Semrock). The fluorescence intensity was detected by using the photomultiplier tube with the counter (53131A, Agilent). The flow cell made with PDMS sheet (volume of 80 μL) was attached to the sensor surface in order to flow the aqueous solutions. The aqueous solution including samples and buffer was flowed over the sensor surface by using peristaltic pump with a flow rate of 0.1 mL/min. The optical setup was controlled by the software Wasplas developed at the Max Planck Institute for Polymer Research (MPIP) in Mainz, Germany. The measured SPR curves taken as the angular reflectivity spectra were fitted by the WinSpall software developed in MPIP.

Detection Assay

For the detection of IL-6, a sandwich immunoassay with fluorescently labeled detection antibody was employed. The immobilization of anti IL-6 capture antibody was performed *in-situ*. After the sensor chip coated with PDA was mounted to the flow cell and the prism head, the sensor surface was made in contact with PBS. The capture antibodies were directly attached to the sensor surface by flowing a solution containing the capture antibody (clone MQ2-13A5) at a concentration of 15 μg/mL in PBS for 70 min, followed by rinsing with PBS for 10 min. The samples containing IL-6 was prepared in PBST with the various concentrations from 100 fM to 100 nM. The solution containing IL-6 was brought in contact to the sensor surfaces for 20 min. Then, the surface was rinsed with PBST for 5 min. The concentration of the detection antibody labeled with fluorophores was adjusted to be 10 nM in PBST, and flowed over the sensor surfaces for 10 min, followed by rinsing with PBST for 5 min.

RESULTS and DISCUSSION

Adsorption of Capture Antibodies on PDA Coated Sensor Surface

Firstly, the adsorption of the capture antibodies (c-Ab) on the PDA coated sensor chips was observed. Before immobilizing the capture antibodies on to the sensor surface, the thickness of the PDA layer was estimated by SPR spectroscopy. Angular reflectivity spectra were taken in PBS before and after PDA coating as shown in the Figure S2 in the supporting information. By fitting the SPR curves, the accumulated PDA layer on the sensor surface was determined to be 1.5 nm in PBS assuming the refractive index of PDA is 1.5. This estimated thickness is in good agreement with the reported value.[26] For the immobilization of capture antibody, a solution containing 15 μg/mL of capture antibody in PBS was brought in contact to the sensor surface for 70 min, followed by rinsing with PBS for 10 min. Figure 2a shows the angular reflectivity spectra taken before and after binding of the capture antibody in PBS. Before immobilization of the capture antibody, a dip in the reflectivity spectrum was observed around θ=57 deg associated with the resonantly excitation of surface plasmons. After the adsorption of capture antibody, the resonance dip shifted to the higher angle as the result of the increment of the refractive index in the vicinity of the sensor surface by binding of capture antibody. The time resolved reflectivity measurement was performed in order to observe the adsorption kinetics of the capture antibody onto the PDA coated sensor surface. The angle of incident was set to 56 deg which is slightly lower than the resonant angle in the SPR curve to obtain the linear sensor response against the refractive index changes. As shown in Figure 2b, the reflectivity immediately increased upon the injection of the capture antibody solution and reached to the plateau after 20 min. During the rinsing process, the reflectivity negligibly decreased. It indicates that the adsorption process of the capture antibody on to the PDA coated sensor surface immediately occurred, and the adsorbed proteins were tightly anchored to the surfaces tightly. We employed the incubation time of 70 min for the attachment of capture antibody to make sure that the sensor surface is fully

covered. Although the increment of the reflectivity was not measurable after 30 min from the introduction of capture antibody, the sensor surface needs to be fully covered with capture antibody as the sensitivity of SPFS biosensors is three orders of magnitude higher than that of SPR sensors based on the refractometric detection.[35] The amount of the immobilized capture antibody was estimated by means of the surface mass density by fitting the SPR curves in Figure 2a. The change in the surface mass density can be described as $\Delta\Gamma = (n_h - n_b)\, d_h / (\partial c/\partial n_h)$, where n_h and n_b denote the refractive index of the protein and the buffer, respectively, d_h is the thickness of the protein layer and $\partial c/\partial n_h$ denotes the refractive index increment factor. For the capture antibody, the refractive index of 1.5 and refractive index increment factor of 0.18 were used, respectively.[36, 37] From the SPR curves in Figure 2a, the change in the thickness of the protein layer d_h was obtained. The increment of the surface mass density due to the adsorption of the capture antibody was determined to be 2.5 ± 0.2 ng/mm^2. This value is in the same range obtained with the IgG proteins attached to the gold sensor substrate by using conventional alkanethiol chemistry,[10, 38] suggesting that the capture antibody densely covered the PDA surfaces.

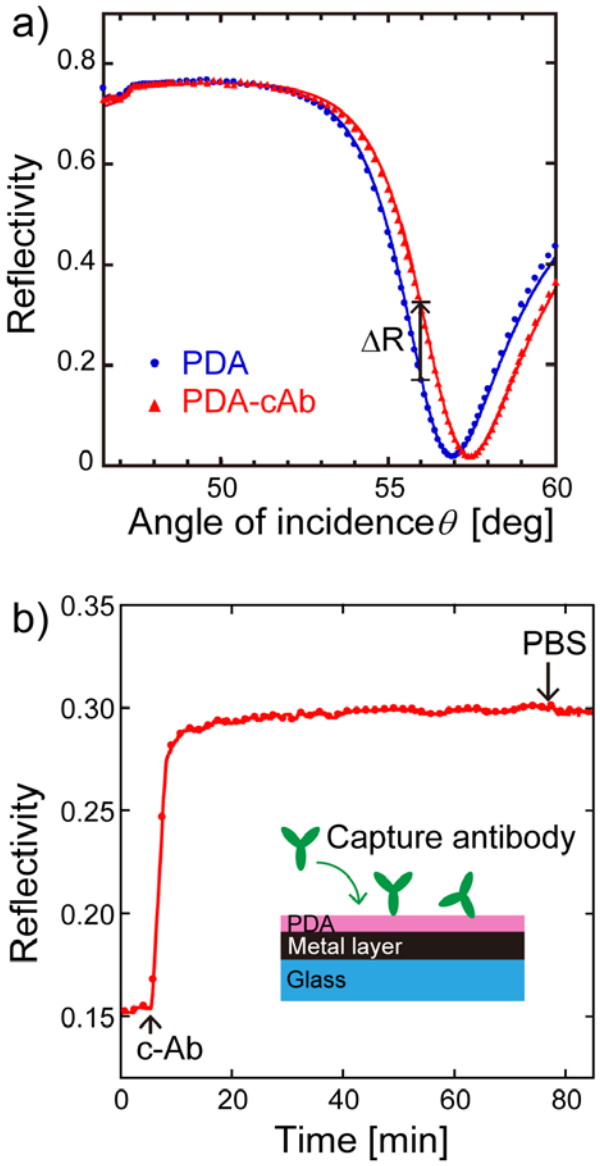

Figure 2. a) SPR curves taken before and after immobilization of capture antibody in PBS. b) Time evolution measurement of reflectivity upon the injection of capture antibody (c-Ab) solution.

Detection of IL-6 by SPFS

In the next experiments, IL-6 was detected by using sandwich assay with SPFS biosensor scheme. Before measuring sensor response at low IL-6 concentration, the sensor response against

the samples containing IL-6 at high concentration was investigated, and compared to that obtained with the blank sample as the control. In this experiment, a sample containing IL-6 at concentration of 100 nM in PBST was flowed over the sensor surface for 20 min, followed by 5 min rinsing with PBST and 10 min flowing of the 10 nM detection antibody (d-Ab) in PBST. The control experiment was performed by injecting the detection antibody directly after the immobilization of the capture antibody, which is corresponding to the blank sample. The angular resolved reflectivity and florescence intensity spectra were taken before and after the injection of the detection antibody for the sample containing IL-6 and the control, see Figure 3a. In contrast to the fact that the resonance angle in the reflectivity spectra didn't exhibit the significant shift, the fluorescence intensity dramatically increased around the resonance angle with the sample containing IL-6 due to the adsorption of the fluorescently labeled detection antibody. The peak of fluorescence intensity around the resonance angle is induced by the enhanced electro-magnetic field in the vicinity of the sensor surface associated with surface plasmon resonance. The increase of the fluorescence intensity was negligible with the control sample with respect to that with the sample containing IL-6. In parallel to the angular resolved measurement, the time evolution of the fluorescence signals ΔF near the resonance angle (θ=56.5 deg) were observed, as shown in Figure 3b. The fluorescence signal ΔF was obtained by subtracting the background signal from the measured fluorescence intensity. For the sample containing IL-6, the fluorescence intensity immediately increased when the detection antibody was introduced, and kept growing until rinsing with PBST. On the other hand, the change of fluorescence intensity was negligible for the control sample not containing IL-6. These results clearly show that the fluorescently labeled detection antibody was adsorbed to IL-6 by affinity bindings, and the protein coated PDA surface hold the anti-fouling properties against the used detection antibody.

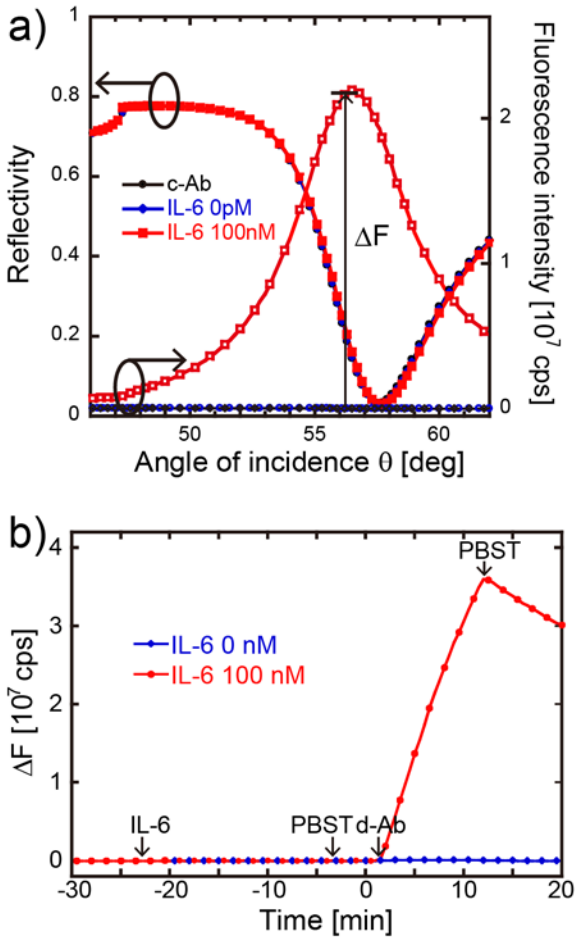

Figure 3. a) Angular resolved reflectivity and fluorescence intensity spectra taken before (black) and after the flow of the detection antibody for the sample containing IL-6 (red), and the control (blue). b) Time evolution of fluorescent signal upon the injections of IL-6 and the detection antibody (d-Ab) in PBST. The angle of incident was set to 56.5 deg.

Calibration Curve for the Detection of IL-6

The calibration curve for the detection of IL-6 with the developed SPFS biosensor was taken, and the limit of detection (LOD) for IL-6 was determined. In the same manner to the previous experiments, samples containing IL-6 at various concentration from 0 pM to 100 pM was introduced to the sensor surface. In order to obtained the comparable sensor response among

different sensor chips, the incident angles were set to slightly lower than the resonance angles where the reflectivity was around 15 %. The same sensor surface was used about three cycles for the detection of IL-6 at the different concentrations. The regeneration of sensor surfaces was performed by flushing 0.1 M HCl solution to remove adsorbed IL-6 and detection antibody, and then rinsing with PBST for 15-20 min. The time evolution of fluorescence intensity shown in Figure S3 in the supporting information revealed that the change in the fluorescence intensity before and after one cycle of the detection assay and the regeneration process was not measurable. Figure 4a shows the real time and *in-situ* measurement of the fluorescence signal ΔF upon the injection of the detection antibody for the samples containing IL-6 at the various concentrations, 0 pM, 0.3 pM, 3 pM and 10 pM. After the detection antibody was introduced to the sensor surface, the fluorescence intensity increased for all the samples including the control, as the detection antibody was brought in the vicinity of the sensor surface where the enhanced electro-magnetic field occurred. For the control sample, the fluorescence intensity dropped immediately to around the baseline by rinsing the sensor surface with PBST. For the samples containing IL-6, the increment of the fluorescence signals was enlarged as the concentration of the IL-6 increased, and the fluorescence signals slowly decreased after the quick intensity drop in the first few minutes by rinsing the surface with PBST. The gradual changes of the fluorescence signals for the samples containing IL-6 was associated with the association and dissociation processes of d-Ab to IL-6 on the sensor surface. The angular resolved reflectivity and fluorescence signal ΔF spectra were taken for the corresponding samples, see Figure 4b. In this plot, the background intensity taken before injection of d-Ab was subtracted from the actual fluorescence intensity in order to eliminate the feature of the background spectrum. The

fluorescence signals exhibited the peaks around the resonance angles, and enhanced as the concentration of IL-6 increased.

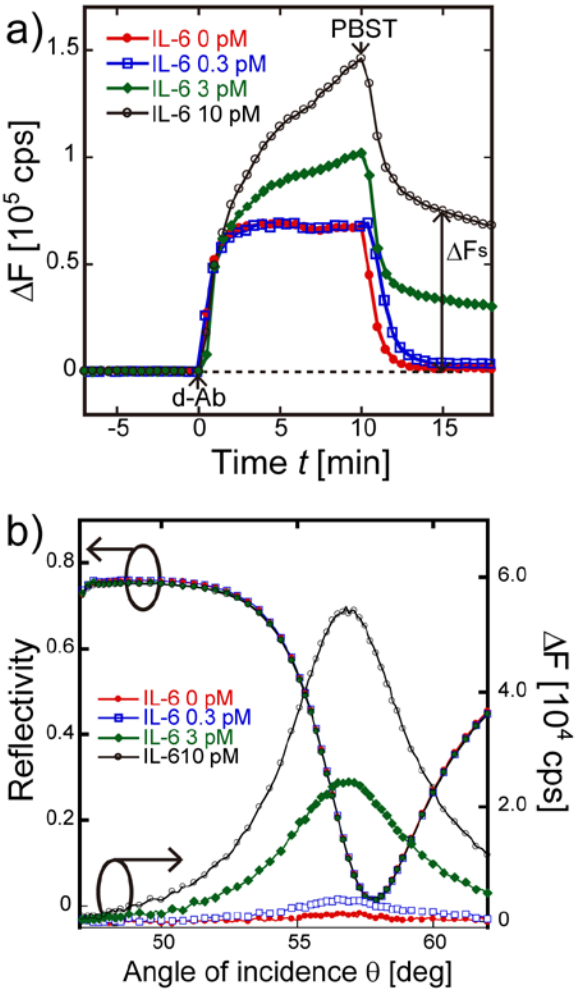

Figure 4. a) Real time, in-situ measurement of fluorescence intensity upon the injection of detection antibody after the flow of the samples containing IL-6 at various concentrations, 0 pM (red), 0.3 pM (blue), 3 pM (green) and 10 pM (black). b) The corresponding angular resolved reflectivity and fluorescence signal spectra taken after the flow of the detection antibody.

The calibration curve for the detection of IL-6 was obtained by plotting the fluorescence signal after 5 min from rinsing with PBST indicated as ΔF_s in Figure 4a as a function of the

concentration of IL-6, see Figure 5. The error bars associating with the variation of the sensor response among the different sensor chips was obtained by repeating the experiment more than three times with different sensor chips. The plotted logarithmic graph shows the linear sensor response against the IL-6 concentration for the investigated concentration range from 100 fM to 100 pM. The small fluorescence signals (ΔF_s =845 ± 125 cps) were observed for the control sample (concentration of IL-6=0 pM), which were induced by the non-specific binding of the detection antibody. The sensor response for the non-specific binding was evaluated with the sensor surface blocked by a solution containing bovine serum in PBS for 10 min incubation time, and the comparable sensor response for the non-specific binding was obtained. Therefore, we attributed the observed non-specific binding without using blocking agent to the physisorption of the detection antibody rather than the covalent attachment to the PDA coated sensor surface. These observations revealed that the low non-specific binding property of the PDA coated sensor surface functionalized with capture antibody by forming densely packed protein layer on the PDA surface. The limit of detection (LOD) for IL-6 was obtained from the intersection between the fitted curve of the sensor response and the sum of the fluorescence signal induced by the non-specific binding and the three times of the standard deviation of the fluorescence intensity. The LOD for the IL-6 was determined to be 100 fM (2 pg/mL) which is in the range of the diagnostic criteria. The obtained LOD for IL-6 was comparable to that measured by another SPFS biosensor utilizing the plasmonic chip with silane coupling agent.[8] By using other sensing schemes such as FET based biosensor and ELISA technique, the similar LOD for IL-6was reported.[39, 40] We consider that the reasonable LOD for IL-6 was obtained in this work compared to that reported previous works, though the LOD is affected by the detection time, the plasmon mode as well as the surface architectures. In addition to the detection sensitivity, the stability and fouling

property of the sensor surface are the important characteristics of the sensor surfaces. In this study, the PDA coated sensor surface was kept in the vacuum desiccator for a couple of weeks before use and any deterioration of the sensing performance was not observed. During the detection process of IL-6, measurable changes were not observed by the regeneration of the sensor surface by hydrochloride. These experimental observations indicate that the PDA coated sensor surfaces are reasonably stable with respect to the conventional thiol chemistry.[41] Regarding the fouling properties of the sensor surface, although noticeable non-specific adsorption of the detection antibody was not detected with the developed sensor surface, adsorption of bovine serum was observed by real-time reflectivity measurement when the blocking of the sensor surfaces was performed. It indicates that the anti-fouling properties of the PDA coated surfaces may need to be improved to be used with a complex media such as plasma and serum by employing backfill chemistry e.g. polyethylene glycol and zwitterionic polymers.[42]

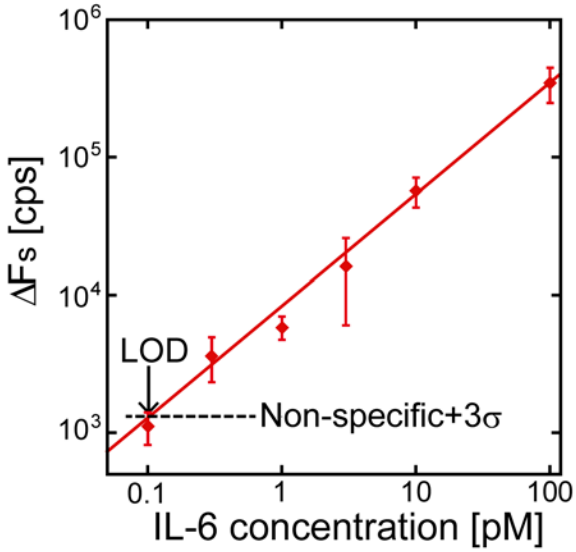

Figure 5. Calibration curve for the detection of IL-6 plotting the fluorescence signals as a function of the IL-6 concentration. The limit of detection (LOD) is indicated where the fitted

curve meets the cut-off value determined by the fluorescence signals associated with the non-specific binding and the standard deviation.

CONCLUSIONS

This paper describes the employment of polydopamine (PDA) thin films as the linker layer for the immobilization of the capture antibody onto the gold surface, and the sensitive detection of the cytokine marker Interleukin-6 (IL-6) by using sandwich assay format and surface plasmon enhanced fluorescence spectroscopy (SPFS). The PDA coated sensor surface was prepared by simply applying a droplet of dopamine solution onto the gold surface with an extremely short incubation time of 10 min. The anti IL-6 capture antibody was directly attached to the PDA coated sensor surface without using any coupling agent and pretreatment. The real time, *in-situ* measurement of the adsorption kinetics of the capture antibody onto the sensor surface revealed that the immobilization of capture antibody immediately occurred, and the sufficient amount of the capture antibody was attached onto the sensor surface compared to that on the sensor surface modified by the conventional thiol chemistry. The fabricated sensor chip exhibited the sensitive sensor response for the samples containing IL-6 by SPFS measurement, with negligible non-specific binding of the detection antibody without using any blocking agent. The detection limit for IL-6 was determined to be 100 fM (2 pg/mL) with the developed SPFS biosensor, which is within the range of the clinical relevant value (1-5 pg/mL). As the resultant LOD for the detection of IL-6 is comparable to that reported by previous works, the utility of the developed sensor chip functionalized with PDA for SPFS biosensor schemes was clearly shown. We believe that the presented surface functionalization method based on PDA coating opens up a new way for the modification of the metallic sensor surfaces with protein molecules, with a simple, brief and inexpensive way without losing the detection sensitivity. Our feature work will

include coating the plasmonic chip with PDA films to create inexpensive and disposable sensor chips for SPFS biosensors and characterizing the sensing performance with complex media such as target molecules in serum.

ASSOCIATED CONTENT

The schematic drawing of sensor instrument, SPR curves taken before and after the deposition of PDA layer on the sensor surface, time evolution of the fluorescence intensity during the regeneration process are provided in the supporting information. This material is available free of charge via the Internet at http://pubs.acs.org.

AUTHOR INFORMATION

Corresponding Author

*ktawa@kwansei.ac.jp.

Author Contributions

The manuscript was written through contributions of all authors. All authors have given approval to the final version of the manuscript.

REFERENCES

1. Turner, A. P. F., Biosensors: Sense and Sensibility. *Chem. Soc. Rev.* **2013,** *42* (8), 3184-3196.
2. Bauch, M.; Toma, K.; Toma, M.; Zhang, Q.; Dostalek, J., Plasmon-Enhanced Fluorescence Biosensors: a Review. *Plasmonics* **2014,** *9* (4), 781-799.
3. Cao, S.-H.; Cai, W.-P.; Liu, Q.; Li, Y.-Q., Surface Plasmon-Coupled Emission: What Can Directional Fluorescence Bring to the Analytical Sciences? *Annu. Rev. Anal. Chem.* **2012,** *5*(5), 317-336.

4. Wang, Y.; Brunsen, A.; Jonas, U.; Dostalek, J.; Knoll, W., Prostate Specific Antigen Biosensor Based on Long Range Surface Plasmon-Enhanced Fluorescence Spectroscopy and Dextran Hydrogel Binding Matrix. *Anal. Chem.* **2009,** *81* (23), 9625-9632.
5. Tawa, K.; Kondo, F.; Sasakawa, C.; Nagae, K.; Nakamura, Y.; Nozaki, A.; Kaya, T., Sensitive Detection of a Tumor Marker, alpha-Fetoprotein, with a Sandwich Assay on a Plasmonic Chip. *Anal. Chem.* **2015,** *87* (7), 3871-3876.
6. Tawa, K.; Umetsu, M.; Nakazawa, H.; Hattori, T.; Kumagai, I., Application of 300x Enhanced Fluorescence on a Plasmonic Chip Modified with a Bispecific Antibody to a Sensitive lmmunosensor. *ACS Appl. Mater. Interfaces* **2013,** *5* (17), 8628-8632.
7. Tawa, K.; Satoh, M.; Uegaki, K.; Hara, T.; Kojima, M.; Kumanogoh, H.; Aota, H.; Yokota, Y.; Nakaoki, T.; Umetsu, M.; Nakazawa, H.; Kumagai, I., Rapid and Sensitive Detection of Brain-Derived Neurotrophic Factor with a Plasmonic Chip. *Jpn. J. Appl. Phys.* **2013,** *52* (6).
8. Tsuneyasu, M.; Sasakawa, C.; Naruishi, N.; Tanaka, Y.; Yoshida, Y.; Tawa, K., Sensitive Detection of Interleukin-6 on a Plasmonic Chip by Grating-Coupled Surface-Plasmon-Field-Enhanced Fluorescence Imaging. *Jpn. J. Appl. Phys.* **2014,** *53* (6).
9. Scholten, A.; Menges, B.; Juebner, M.; Rothschild, M. A.; Bender, K., A Mixed Alkanethiol Based Immunosensor for Surface Plasmon Field-Enhanced Fluorescence Spectroscopy in Serum. *Analyst* **2013,** *138* (6), 1705-1712.
10. Huang, C.-J.; Dostalek, J.; Sessitsch, A.; Knoll, W., Long-Range Surface Plasmon-Enhanced Fluorescence Spectroscopy Biosensor for Ultrasensitive Detection of E. coli O157:H7. *Anal. Chem.* **2011,** *83* (3), 674-677.
11. Chang, Y. F.; Tsao, K. C.; Liu, Y. C.; Chen, Y. C.; Yu, P. C.; Huang, Y. C.; Chou, C., Diagnosis of Human Metapneumovirus in Patients Hospitalized with Acute Lower Respiratory Tract Infection Using a Metal-Enhanced Fluorescence Technique. *J. Virol. Methods* **2015,** *213*, 151-156.
12. Wang, Y.; Dostalek, J.; Knoll, W., Long Range Surface Plasmon-Enhanced Fluorescence Spectroscopy for the Detection of Aflatoxin M-1 in Milk. *Biosens. Bioelectron.* **2009,** *24* (7), 2264-2267.
13. Park, H.; Germini, A.; Sforza, S.; Corradini, R.; Marchelli, R.; Knoll, W., Kinetic and Affinity Analyses of Hybridization Reactions Between Peptide Nucleic Acid Probes and DNA Targets Using Surface Plasmon Field-Enhanced Fluorescence Spectroscopy. *Biointerphases* **2006,** *1* (4), 113-122.
14. Wang, J.; Zhou, H. S., Aptamer-Based Au Nanoparticles-Enhanced Surface Plasmon Resonance Detection of Small Molecules. *Anal. Chem.* **2008,** *80* (18), 7174-7178.
15. Matsuura, R.; Tawa, K.; Kitayama, Y.; Takeuchi, T., A Plasmonic Chip-Based Bio/chemical Hybrid Sensing System for the Highly Sensitive Detection of C-reactive Protein. *Chem. Commun.* **2016,** *52* (20), 3883-3886.
16. Ye, L.; Haupt, K., Molecularly imprinted polymers as antibody and receptor mimics for assays, sensors and drug discovery. *Anal. Bioanal. Chem.* **2004,** *378* (8), 1887-1897.
17. Lahiri, J.; Isaacs, L.; Tien, J.; Whitesides, G. M., A Strategy for the Generation of Surfaces Presenting Ligands for Studies of Binding Based on an Active Ester as a Common Reactive Intermediate: A Surface Plasmon Resonance Study. *Anal. Chem.* **1999,** *71* (4), 777-790.
18. Neumann, T.; Johansson, M. L.; Kambhampati, D.; Knoll, W., Surface-Plasmon Fluorescence Spectroscopy. *Adv. Funct. Mater.* **2002,** *12* (9), 575-586.

19. Vareiro, M. L. M.; Liu, J.; Knoll, W.; Zak, K.; Williams, D.; Jenkins, A. T. A., Surface Plasmon Fluorescence Measurements of Human Chorionic Gonadotrophin: Role of Antibody Orientation in Obtaining Enhanced Sensitivity and Limit of Detection. *Anal. Chem.* **2005,** *77* (8), 2426-2431.
20. Chang, Y. F.; Hung, S. H.; Lee, Y. J.; Chen, R. C.; Su, L. C.; Lai, C. S.; Chou, C., Discrimination of Breast Cancer by Measuring Prostate-Specific Antigen Levels in Women's Serum. *Anal. Chem.* **2011,** *83* (13), 5324-5328.
21. Pleschberger, M.; Saerens, D.; Weigert, S.; Sleytr, U. B.; Muyldermans, S.; Sara, M.; Egelseer, E. M., An S-layer Heavy Chain Camel Antibody Fusion Protein for Generation of a Nanopatterned Sensing Layer to Detect the Prostate-Specific Antigen by Surface Plasmon Resonance Technology. *Bioconjugate Chem.* **2004,** *15* (3), 664-671.
22. Lee, H.; Dellatore, S. M.; Miller, W. M.; Messersmith, P. B., Mussel-Inspired Surface Chemistry for Multifunctional Coatings. *Science* **2007,** *318* (5849), 426-430.
23. Rodriguez-Emmenegger, C.; Preuss, C. M.; Yameen, B.; Pop-Georgievski, O.; Bachmann, M.; Mueller, J. O.; Bruns, M.; Goldmann, A. S.; Bastmeyer, M.; Barner-Kowollik, C., Controlled Cell Adhesion on Poly(dopamine) Interfaces Photopatterned with Non-Fouling Brushes. *Adv. Mater.* **2013,** *25* (42), 6123-6127.
24. Toma, M.; Loget, G.; Corn, R. M., Flexible Teflon Nanocone Array Surfaces with Tunable Superhydrophobicity for Self-Cleaning and Aqueous Droplet Patterning. *ACS Appl. Mater. Interfaces* **2014,** *6* (14), 11110-11117.
25. Ren, J.; Han, P.; Wei, H.; Jia, L., Fouling-Resistant Behavior of Silver Nanoparticle-Modified Surfaces against the Bioadhesion of Microalgae. *ACS Appl. Mater. Interfaces* **2014,** *6* (6), 3829-3838.
26. Wood, J. B.; Szyndler, M. W.; Halpern, A. R.; Cho, K.; Corn, R. M., Fabrication of DNA Microarrays on Polydopamine-Modified Gold Thin Films for SPR Imaging Measurements. *Langmuir* **2013,** *29* (34), 10868-10873.
27. Shi, S.; Wang, L.; Su, R.; Liu, B.; Huang, R.; Qi, W.; He, Z., A Polydopamine-Modified Optical Fiber SPR Biosensor Using Electroless-Plated Gold Films for Immunoassays. *Biosens. Bioelectron.* **2015,** *74*, 454-460.
28. Lynge, M. E.; van der Westen, R.; Postma, A.; Stadler, B., Polydopamine-a Nature-Inspired Polymer Coating for Biomedical Science. *Nanoscale* **2011,** *3* (12), 4916-4928.
29. Loget, G.; Wood, J. B.; Cho, K.; Halpern, A. R.; Corn, R. M., Electrodeposition of Polydopamine Thin Films for DNA Patterning and Microarrays. *Anal. Chem.* **2013,** *85* (21), 9991-9995.
30. Hack, C. E.; Degroot, E. R.; Feltbersma, R. J. F.; Nuijens, J. H.; Vanschijndel, R.; Eerenbergbelmer, A. J. M.; Thijs, L. G.; Aarden, L. A., Increased Plasma-Levels of Interleukin-6 in Sepsis. *Blood* **1989,** *74* (5), 1704-1710.
31. Yoshizaki, K.; Matsuda, T.; Nishimoto, N.; Kuritani, T.; Taeho, L.; Aozasa, K.; Nakahata, T.; Kawai, H.; Tagoh, H.; Komori, T.; Kishimoto, S.; Hirano, T.; Kishimoto, T., Pathogenic Significance of Interleukin-6 (IL-6/BSF-2) in Castlemans Disease. *Blood* **1989,** *74* (4), 1360-1367.
32. Jones, S. A.; Scheller, J.; Rose-John, S., Therapeutic Strategies for the Clinical Blockade of IL-6/gp130 Signaling. *J. Clin. Invest.* **2011,** *121* (9), 3375-3383.
33. Ridker, P. M.; Rifai, N.; Stampfer, M. J.; Hennekens, C. H., Plasma Concentration of Interleukin-6 and the Risk of Future Myocardial Infarction Among Apparently Healthy Men. *Circulation* **2000,** *101* (15), 1767-1772.

34. Toma, M.; Cho, K.; Wood, J. B.; Corn, R. M., Gold Nanoring Arrays for Near Infrared Plasmonic Biosensing. *Plasmonics* **2014,** *9* (4), 765-772.
35. Liebermann, T.; Knoll, W., Surface-plasmon Field-Enhanced Fluorescence Spectroscopy. *Colloids Surf., A* **2000,** *171* (1-3), 115-130.
36. Voros, J., The Density and Refractive Index of Adsorbing Protein Layers. *Biophys. J.* **2004,** *87* (1), 553-561.
37. Tumolo, T.; Angnes, L.; Baptista, M. S., Determination of the Refractive Index Increment (dn/dc) of Molecule and Macromolecule Solutions by Surface Plasmon Resonance. *Anal. Biochem.* **2004,** *333* (2), 273-279.
38. Wang, Y.; Huang, C. J.; Jonas, U.; Wei, T. X.; Dostalek, J.; Knoll, W., Biosensor Based on Hydrogel Optical Waveguide Spectroscopy. *Biosens. Bioelectron.* **2010,** *25* (7), 1663-1668.
39. Huang, J. F.; Chen, H.; Niu, W. B.; Fam, D. W. H.; Palaniappan, A.; Larisika, M.; Faulkner, S. H.; Nowak, C.; Nimmo, M. A.; Liedberg, B.; Tok, A. I. Y., Highly Manufacturable Graphene Oxide Biosensor for Sensitive Interleukin-6 Detection. *Rsc Advances* **2015,** *5* (49), 39245-39251.
40. Helle, M.; Boeije, L.; Degroot, E.; Devos, A.; Aarden, L., Sensitive ELISA for Interleukin-6: Detection of IL-6 in Biological Fluids: Synovial Fluids and Sera. *J. Immunol. Methods* **1991,** *138* (1), 47-56.
41. Jans, K.; Bonroy, K.; De Palma, R.; Reekmans, G.; Jans, H.; Laureyn, W.; Smet, M.; Borghs, G.; Maes, G., Stability of Mixed PEO-thiol SAMs for Biosensing Applications. *Langmuir* **2008,** *24* (8), 3949-3954.
42. Jiang, S. Y.; Cao, Z. Q., Ultralow-Fouling, Functionalizable, and Hydrolyzable Zwitterionic Materials and Their Derivatives for Biological Applications. *Adv. Mater.* **2010,** *22* (9), 920-932.

Table of Contents Graphic

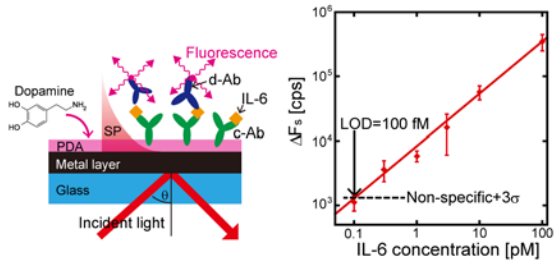

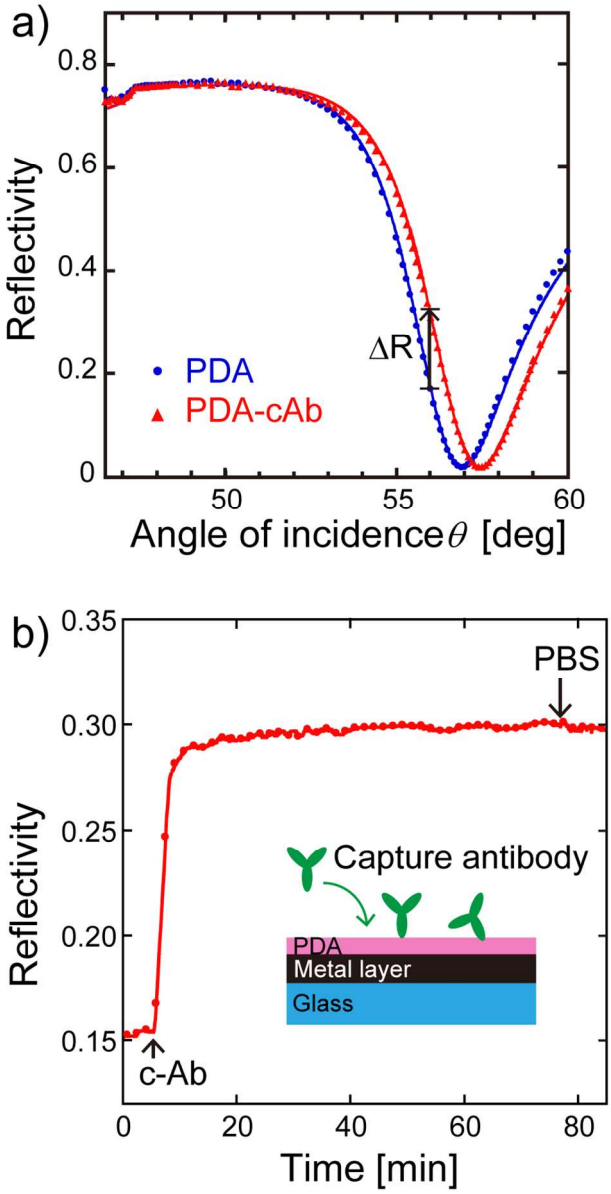

Figure 2. a) SPR curves taken before and after immobilization of capture antibody in PBS for 70 min. b) Time evolution measurement of reflectivity upon the injection of capture antibody (c-Ab) solution.
Figure 2
77x150mm (300 x 300 DPI)

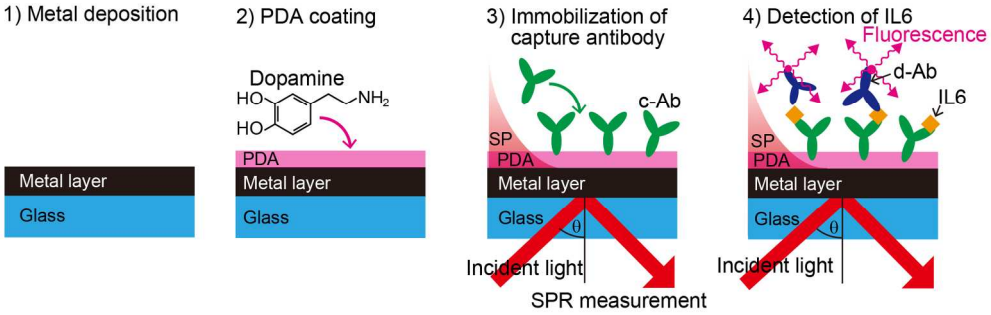

Figure 1. Sample preparation scheme. 1) Deposition of a gold thin film. 2) PDA coating. 3) Immobilization of capture antibody. 4) Detection of IL-6 by sandwich assay with fluorophore labeled detection antibody.
Figure 1
173x54mm (300 x 300 DPI)

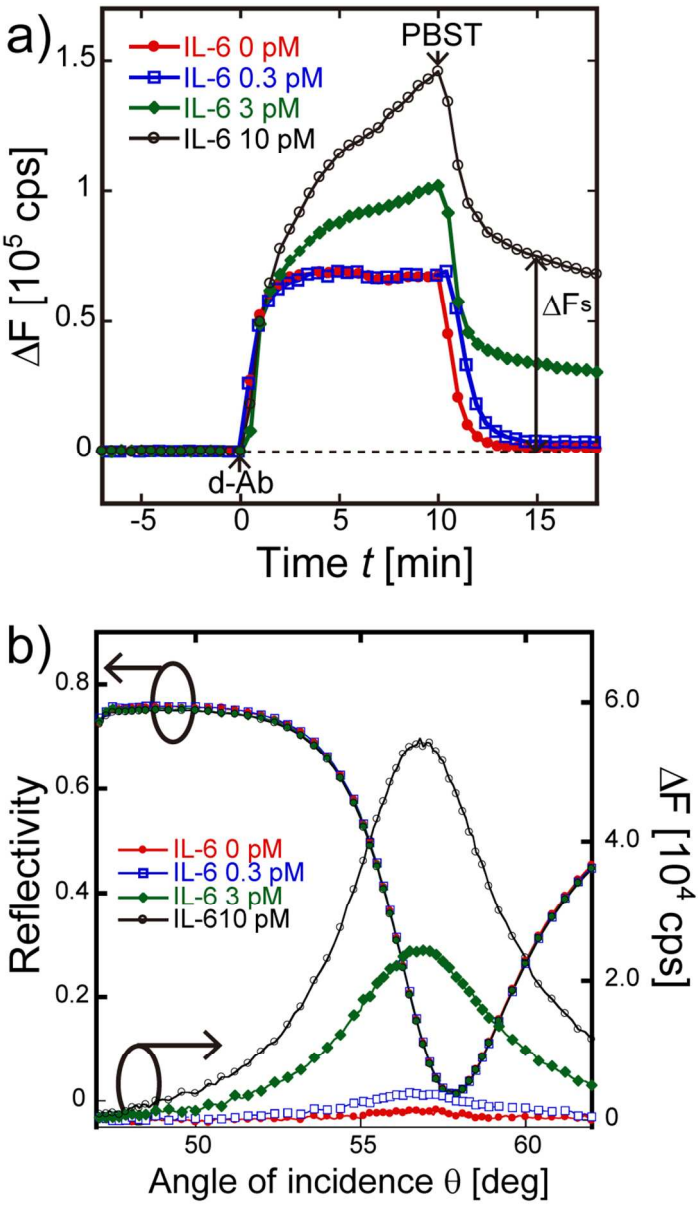

Figure 4. a) Real time, in-situ measurement of fluorescence intensity and upon the injection of detection antibody after the flow of the samples containing IL-6 at various concentrations, 0 pM (red), 0.3 pM (blue), 3 pM (green) and 10 pM (black). b) The corresponding angular resolved reflectivity and fluorescence signal spectra taken after the flow of the detection antibody.

Figure 4
78x133mm (300 x 300 DPI)

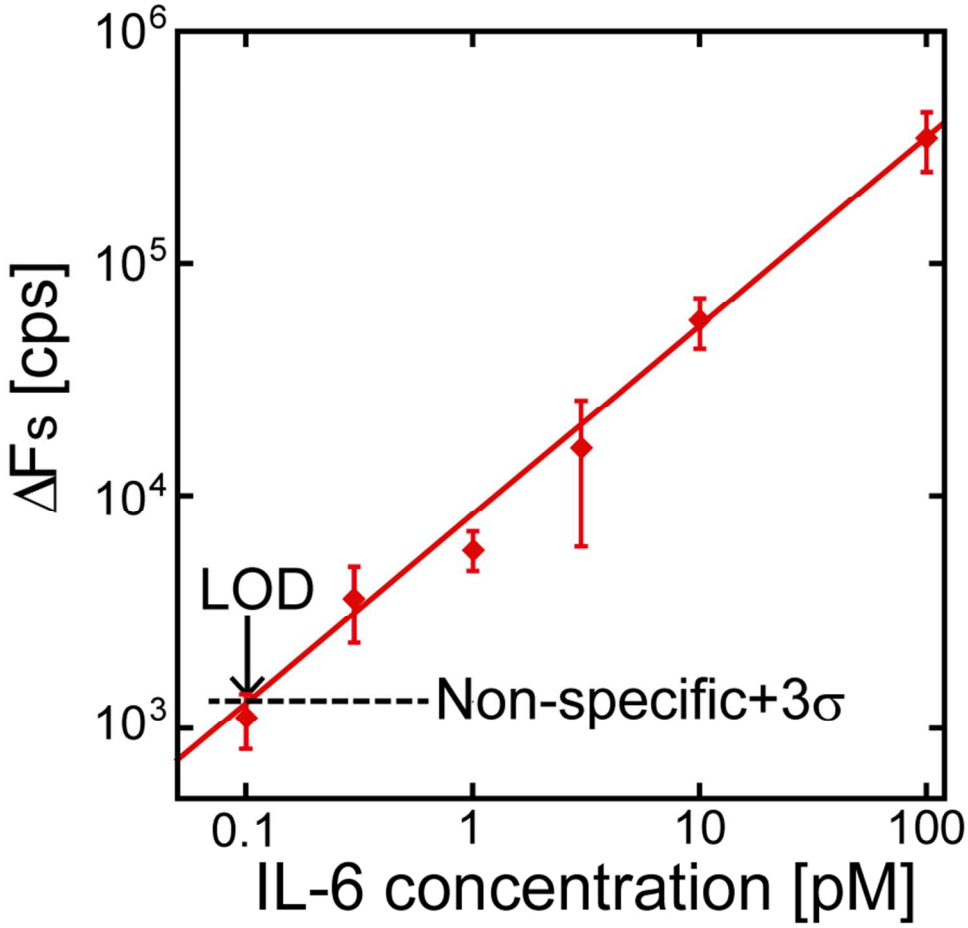

Figure 5. Calibration curve for the detection of IL-6 plotting the fluorescence signals as a function of the IL-6 concentration. The limit of detection (LOD) is indicated where the fitted curve meets the cut-off value determined by the fluorescence signals associated with the non-specific binding and the standard deviation.
Figure 5
78x73mm (300 x 300 DPI)